ISA Transactions xxx (xxxx) xxx

Contents lists available at ScienceDirect

ISA Transactions

journal homepage: www.elsevier.com/locate/isatrans

Research article

Observer-based finite frequency $H\infty$ state-feedback control for autonomous ground vehicles☆

Heng Wang [a], Wenwen Song [a], Yongyu Liang [a], Qing Li [a,b,*], Deyu Liang [a]

[a] School of Automation and Electrical Engineering, Key Laboratory of Knowledge Automation for Industrial Processes of Ministry of Education, University of Science and Technology Beijing, Beijing, 100083, PR China

[b] Shunde Graduate School of University of Science and Technology Beijing, Foshan, Guangdong, 528300, PR China

ARTICLE INFO

Article history:
Received 27 August 2020
Received in revised form 16 March 2021
Accepted 16 March 2021
Available online xxxx

Keywords:
Path following
Observer-based
Finite frequency
H_∞ performance

ABSTRACT

This paper studies the problem of path tracking of Autonomous Ground Vehicles (AGVs) in the presence of sideslip angles. An observer is designed to estimate both the sideslip angle and the vehicle yaw rate, based on which an observer-based controller is established such that the closed-loop system is stable and the vehicle follows a desired path accurately. In particular, the nonlinear vehicle dynamics model is reformulated as a Linear Parameter Varying (LPV) system, and a finite frequency H_∞ criteria is satisfied such that the disturbances are attenuated effectively, the parameter-dependent gain matrices are calculated simultaneously by solving a convex optimization problem. Simulation results show the effectiveness of the method proposed.

1. Introduction

Path tracking control is one of the essential tasks of autonomous ground vehicles (AGVs), which requires that the vehicle travel along desired paths, a lot of related research has been presented in the literature [1,2]. It has been well known that PID control has been widely used due to its advantages in dealing with complex systems with nonlinear and uncertain parameters and structures [3]. By combining with other techniques such as fuzzy methods etc., the performance of PID control method can be improved greatly when applied to path tracking control problems for AGVs [4], and model predictive control (MPC) is another common method for path following controller design when different constraints are considered [5,6].

Particularly, in [7], convex quadratic programming (CQP) techniques are used to deal with the constraints of MPC for collision-free navigation of autonomous vehicles, and in [8], two independent model predictive controllers are designed for longitudinal and lateral motion planning, respectively. In addition, preview control, sliding mode control and adaptive control strategies are also common control methods for path tracking [9–12]. To enhance system robustness, the nonsingular terminal sliding mode control is combined with active disturbance rejection control in [13], and an advanced event-triggered communication scheme is proposed in [14]. In [15], a robust steering control method is presented by the aid of a neural network approximator. On the other hand, $H\infty$ control is also widely utilized to improve the system robustness [16]. In [17], a robust path tracking control strategy is proposed for AGVs with data loss and delay, and in [18], a switching $H\infty$ optimal control method is proposed.

In practice, the frequencies of disturbances are usually bounded and their ranges are generally known, for systems with finite frequency external disturbances, the design of robust controllers in finite frequency domain instead of full frequency domain may receive better performance in both stability and robustness aspects. For example, an integrated design approach called generalized KYP lemma is proposed in [19], where the classical KYP lemma is generalized to finite frequency cases, and the conservatism introduced by full frequency design methods is reduced greatly. In [20,21], finite frequency design methods have been used for vehicle systems with and without faults, respectively. Note that AGV systems are usually approximated by linear systems affected by disturbances, model uncertainties, and faults etc [22–25]. In particular, in [26–28], nonlinear systems are converted into LPV systems, and parameter-dependent gains are obtained by the aid of parameter-dependent Lyapunov functions and linear matrix inequality (LMI) techniques. Further, state measurements including positions and headings are apt to

☆ This work has been supported in part by the Funds of National Natural Science Foundation of China (Grant Nos. 61673098), Scientific and Technological Innovation Foundation of Shunde Graduate School, USTB, China (Grant No. BK19BE022), and the Fundamental Research Funds for the Central Universities, China (Grant Nos. FRF-DF-20-35, FRF-BD-19-002A).

* Corresponding author at: School of Automation and Electrical Engineering, Key Laboratory of Knowledge Automation for Industrial Processes of Ministry of Education, University of Science and Technology Beijing, Beijing, 100083, PR China.

E-mail address: liqing@ies.ustb.edu.cn (Q. Li).

https://doi.org/10.1016/j.isatra.2021.03.027
0019-0578/

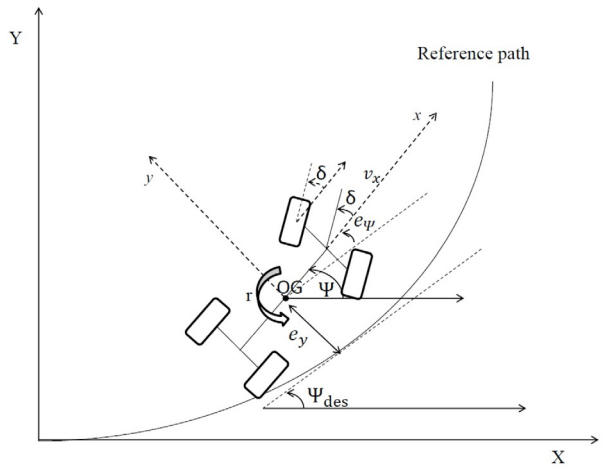

Fig. 1. Schematic diagram of path tracking model.

be affected by external disturbances, which will affect the path tracking performance obviously. To deal with this issue, different state estimation approaches have been proposed [29,30], and in [31], an adaptive neural network control method is designed for a kind of remotely operated vehicles. In [32], a dynamic output feedback steering control method is proposed based on the design of a fuzzy observer. In [33], a robust sliding-mode observer is proposed for an LPV system affected by external disturbances and unknown inputs etc.

In this paper, a path tracking controller is designed through estimating both the sideslip angle and yaw rate. The main contribution of the paper is twofold. Firstly, the vehicle model is reformulated as an LPV system, an observer is designed which is used to estimate both the sideslip angle and yaw rate of the vehicle, and a state feedback controller is designed to guarantee that the closed-loop system meets certain finite frequency performance index such that the disturbances are suppressed effectively compared to the classic full frequency approaches. Secondly, both the observer and controller gains are parameter-dependent and are obtained by solving a set of LMIs simultaneously. Simulation results illustrate the effectiveness of the controller designed, where desired paths are tracked with satisfactory performance in spite of the influence of external disturbances. The paper is arranged as follows. The vehicle model and problem formulation are presented in Section 2. The detailed design conditions for controller and observer are given in Section 3. The stability conditions are analyzed in Section 4, simulation results and some conclusions are provided in Section 5 and Section 6, respectively.

Notation:. Throughout this paper, I is used to represent an identity matrix. $diag\{Y_1, Y_2, \ldots, Y_n\}$ denotes a block diagonal matrix, whose main diagonal matrices are $Y_1, Y_2, \ldots, Y_n$. A^T denotes the transpose of a matrix A, $He(A)$ means $A + A^*$. $A < 0 (\leqslant 0)$ means that A is negative (semi) definiteness.

2. Problem formulation

Consider a two degree-of-freedom vehicle model, the schematic diagram of path tracking is shown in Fig. 1, where r denotes the yaw rate, e_y denotes the lateral offset between vehicle and the desired path, and e_ψ denotes heading error, and they can be measured by onboard sensors e.g., Inertial Measurement Unit (IMU) etc. v_x and v_y denote the longitudinal and lateral velocities of vehicle which are both measurable, δ denotes steering angle.

Let e_y and e_ψ denote the tracking errors of path and heading angle respectively, similar to [17], we have that

$$\begin{cases} \dot{e}_y = v_x\beta + v_x e_\psi + d_1 \\ \dot{e}_\psi = r - \rho v_x \end{cases} \tag{1}$$

where β is vehicle sideslip angle, r denotes yaw rate of vehicle, ρ represents the curvature at the desired path, d_1 represents external disturbances.

Further, note that

$$\begin{cases} \dot{\beta} = \frac{1}{mv_x}(F_{yf} + F_{yr}) - r + d_3 \\ \dot{r} = \frac{1}{I_z}(l_f F_{yf} - l_r F_{yr}) + \frac{1}{I_z} d_4 \end{cases} \tag{2}$$

where m denotes vehicle mass, I_z is inertia, l_f and l_r are distances from the center of the front and rear axle wheel to the center of gravity of vehicle, respectively. F_{yf} and F_{yr} denote the lateral forces of front and rear wheels, respectively.

$$F_{yf} = C_f\alpha_f, F_{yr} = C_r\alpha_r \tag{3}$$

where C_f and C_r denote the cornering stiffness wheels, and α_f and α_r denote slip angles.

Combining (1)–(3), we have

$$\begin{cases} \dot{e}_y = v_x\beta + v_x e_\psi + d_1 \\ \dot{e}_\psi = r + v_x d_2 \\ \dot{\beta} = a_{11}\beta + a_{12} r + b_1\delta + d_3 \\ \dot{r} = a_{21}\beta + a_{22} r + b_2\delta + \frac{1}{I_z} d_4 \end{cases} \tag{4}$$

where d_2 represents modeling errors, and

$$a_{11} = -\frac{C_f + C_r}{mv_x}, a_{12} = -(1 + \frac{C_f l_f - C_r l_r}{mv_x^2}), a_{21} = \frac{C_r l_r - C_f l_f}{I_z},$$

$$a_{22} = -\frac{C_f l_f^2 + C_r l_r^2}{I_z v_x}, b_1 = \frac{C_f}{mv_x}, b_2 = \frac{C_f l_f}{I_z}$$

Let $x(t) = [e_y, e_\psi, \beta, r]^T$ denote state, and $u(t) = \delta$ denote control input, $d(t) = [d_1(t), d_2(t), d_3(t), d_4(t)]^T$ denote external disturbances, we have that the vehicle model can be denoted as

$$\dot{x}(t) = Ax(t) + Bu(t) + B_d d(t) \tag{5}$$

where system matrices

$$A = \begin{bmatrix} 0 & v_x & v_x & 0 \\ 0 & 0 & 0 & 1 \\ 0 & 0 & a_{11} & a_{12} \\ 0 & 0 & a_{21} & a_{22} \end{bmatrix}, B = \begin{bmatrix} 0 \\ 0 \\ b_1 \\ b_2 \end{bmatrix}, B_d = \text{diag}\{1, v_x, 1, \frac{1}{I_z}\}$$

Assume that v_x varies in the interval $[\underline{v}_x, \overline{v}_x]$, we have that $\frac{1}{v_x} \in [\frac{1}{\overline{v}_x}, \frac{1}{\underline{v}_x}]$, and $\frac{1}{v_x^2} \in [\frac{1}{\overline{v}_x^2}, \frac{1}{\underline{v}_x^2}]$. Define α_i, $i = 1, \ldots, 8$ as

$$\alpha_1 = \frac{|v_x - \overline{v}_x||\frac{1}{v_x} - \frac{1}{\overline{v}_x}||\frac{1}{v_x^2} - \frac{1}{\overline{v}_x^2}|}{|\underline{v}_x - \overline{v}_x||\frac{1}{\underline{v}_x} - \frac{1}{\overline{v}_x}||\frac{1}{\underline{v}_x^2} - \frac{1}{\overline{v}_x^2}|}, \alpha_2 = \frac{|v_x - \overline{v}_x||\frac{1}{v_x} - \frac{1}{\overline{v}_x}||\frac{1}{v_x^2} - \frac{1}{\underline{v}_x^2}|}{|\underline{v}_x - \overline{v}_x||\frac{1}{\underline{v}_x} - \frac{1}{\overline{v}_x}||\frac{1}{\underline{v}_x^2} - \frac{1}{\overline{v}_x^2}|},$$

$$\alpha_3 = \frac{|v_x - \overline{v}_x||\frac{1}{v_x} - \frac{1}{\underline{v}_x}||\frac{1}{v_x^2} - \frac{1}{\underline{v}_x^2}|}{|\underline{v}_x - \overline{v}_x||\frac{1}{\underline{v}_x} - \frac{1}{\overline{v}_x}||\frac{1}{\underline{v}_x^2} - \frac{1}{\overline{v}_x^2}|}, \alpha_4 = \frac{|v_x - \overline{v}_x||\frac{1}{v_x} - \frac{1}{\underline{v}_x}||\frac{1}{v_x^2} - \frac{1}{\underline{v}_x^2}|}{|\underline{v}_x - \overline{v}_x||\frac{1}{\underline{v}_x} - \frac{1}{\overline{v}_x}||\frac{1}{\underline{v}_x^2} - \frac{1}{\overline{v}_x^2}|},$$

$$\alpha_5 = \frac{|v_x - \underline{v}_x||\frac{1}{v_x} - \frac{1}{\overline{v}_x}||\frac{1}{v_x^2} - \frac{1}{\overline{v}_x^2}|}{|\underline{v}_x - \overline{v}_x||\frac{1}{\underline{v}_x} - \frac{1}{\overline{v}_x}||\frac{1}{\underline{v}_x^2} - \frac{1}{\overline{v}_x^2}|}, \alpha_6 = \frac{|v_x - \underline{v}_x||\frac{1}{v_x} - \frac{1}{\overline{v}_x}||\frac{1}{v_x^2} - \frac{1}{\underline{v}_x^2}|}{|\underline{v}_x - \overline{v}_x||\frac{1}{\underline{v}_x} - \frac{1}{\overline{v}_x}||\frac{1}{\underline{v}_x^2} - \frac{1}{\overline{v}_x^2}|},$$

$$\alpha_7 = \frac{|v_x - \underline{v}_x||\frac{1}{v_x} - \frac{1}{\underline{v}_x}||\frac{1}{v_x^2} - \frac{1}{\underline{v}_x^2}|}{|\underline{v}_x - \overline{v}_x||\frac{1}{\underline{v}_x} - \frac{1}{\overline{v}_x}||\frac{1}{\underline{v}_x^2} - \frac{1}{\overline{v}_x^2}|}, \alpha_8 = \frac{|v_x - \underline{v}_x||\frac{1}{v_x} - \frac{1}{\underline{v}_x}||\frac{1}{v_x^2} - \frac{1}{\underline{v}_x^2}|}{|\underline{v}_x - \overline{v}_x||\frac{1}{\underline{v}_x} - \frac{1}{\overline{v}_x}||\frac{1}{\underline{v}_x^2} - \frac{1}{\overline{v}_x^2}|}.$$

we have that (5) can be formulated as an LPV system

$$\dot{x}(t) = A(\alpha)x(t) + B(\alpha)u(t) + B_d(\alpha)d(t) \tag{6}$$

where $A(\alpha)=\sum_{i=1}^{8}\alpha_i A_i$, $B(\alpha)=\sum_{i=1}^{8}\alpha_i B_i$, $B_d(\alpha)=\sum_{i=1}^{8}\alpha_i B_{d,i}$, with $0<\alpha_i<1$, $\sum_{i=1}^{8}\alpha_i=1$, and

$$A_1=\begin{bmatrix}0&\underline{v}_x&\underline{v}_x&0\\0&0&0&1\\0&0&\underline{a}_{11}&\underline{a}_{12}\\0&0&a_{21}&\underline{a}_{22}\end{bmatrix},A_2=\begin{bmatrix}0&\underline{v}_x&\underline{v}_x&0\\0&0&0&1\\0&0&\underline{a}_{11}&\bar{a}_{12}\\0&0&a_{21}&\underline{a}_{22}\end{bmatrix}$$

$$A_3=\begin{bmatrix}0&\underline{v}_x&\underline{v}_x&0\\0&0&0&1\\0&0&\bar{a}_{11}&\bar{a}_{12}\\0&0&a_{21}&\bar{a}_{22}\end{bmatrix},A_4=\begin{bmatrix}0&\underline{v}_x&\underline{v}_x&0\\0&0&0&1\\0&0&\bar{a}_{11}&\underline{a}_{12}\\0&0&a_{21}&\bar{a}_{22}\end{bmatrix}$$

$$A_5=\begin{bmatrix}0&\bar{v}_x&\bar{v}_x&0\\0&0&0&1\\0&0&\underline{a}_{11}&\underline{a}_{12}\\0&0&a_{21}&\underline{a}_{22}\end{bmatrix},A_6=\begin{bmatrix}0&\bar{v}_x&\bar{v}_x&0\\0&0&0&1\\0&0&\underline{a}_{11}&\bar{a}_{12}\\0&0&a_{21}&\underline{a}_{22}\end{bmatrix}$$

$$A_7=\begin{bmatrix}0&\bar{v}_x&\bar{v}_x&0\\0&0&0&1\\0&0&\bar{a}_{11}&\bar{a}_{12}\\0&0&a_{21}&\bar{a}_{22}\end{bmatrix},A_8=\begin{bmatrix}0&\bar{v}_x&\bar{v}_x&0\\0&0&0&1\\0&0&\bar{a}_{11}&\underline{a}_{12}\\0&0&a_{21}&\bar{a}_{22}\end{bmatrix}$$

$$B_1=B_2=B_5=B_6=\begin{bmatrix}0\\0\\\frac{C_f}{m\underline{v}_x}\\\frac{C_f l_f}{I_z}\end{bmatrix},B_3=B_4=B_7=B_8=\begin{bmatrix}0\\0\\\frac{C_f}{m\bar{v}_x}\\\frac{C_f l_f}{I_z}\end{bmatrix}$$

$$B_{d,1}=B_{d,2}=B_{d,3}=B_{d,4}=\mathrm{diag}\{1,\underline{v}_x,1,\frac{1}{I_z}\}$$

$$B_{d,5}=B_{d,6}=B_{d,7}=B_{d,8}=\mathrm{diag}\{1,\bar{v}_x,1,\frac{1}{I_z}\}$$

$$\underline{a}_{11}=-\frac{C_f+C_r}{m\underline{v}_x},\quad \bar{a}_{11}=-\frac{C_f+C_r}{m\bar{v}_x}$$

$$\underline{a}_{12}=-(1+\frac{C_f l_f-C_r l_r}{m\underline{v}_x^2}),\quad \bar{a}_{12}=-(1+\frac{C_f l_f-C_r l_r}{m\bar{v}_x^2})$$

$$\underline{a}_{22}=-\frac{C_f l_f^2+C_r l_r^2}{I_z\underline{v}_x},\quad \bar{a}_{22}=-\frac{C_f l_f^2+C_r l_r^2}{I_z\bar{v}_x}$$

The task of this paper is to design a control strategy such that the closed-loop path tracking system is stable and the disturbances are attenuated effectively. However, the measurement of system states is inevitably affected by noises, an observer is designed for state estimation, and an observer-based state-feedback controller is proposed instead of classic state-feedback controller, such that the desired path is tracked accurately.

Denote $y(t)$ as measurement of state $x(t)$, and let $w(t)$ denote the measurement noise, we have that

$$y(t)=Cx(t)+Dw(t) \tag{7}$$

where C is an identity matrix, and D is a diagonal weighting matrix. Combining (7) and (5), we have

$$\begin{aligned}\dot{x}(t)&=A(\alpha)x(t)+B(\alpha)u(t)+B_d(\alpha)d(t)\\y(t)&=Cx(t)+Dw(t)\end{aligned} \tag{8}$$

Next, the design procedure of observer-based state-feedback controller will be presented in details.

3. Observer-based H∞ state-feedback controller design

Let observer model be

$$\begin{aligned}\dot{\hat{x}}(t)&=A(\alpha)\hat{x}(t)+B(\alpha)u(t)+L(\alpha)(\hat{y}(t)-y(t))\\\hat{y}(t)&=C\hat{x}(t)\end{aligned} \tag{9}$$

where $\hat{x}(t)$ is observer state which is to estimate $x(t)$, $A(\alpha)$ and $B(\alpha)$ are the same as defined in (8), $L(\alpha)$ is a parameter-dependent observer gain matrix.

Define state estimation error $\tilde{x}(t)=\hat{x}(t)-x(t)$, then we have

$$\begin{aligned}\dot{\tilde{x}}(t)&=\dot{\hat{x}}(t)-\dot{x}(t)\\&=A(\alpha)\tilde{x}(t)+L(\alpha)(\hat{y}(t)-y(t))-B_d d(t)\\&=A(\alpha)\tilde{x}(t)+L(\alpha)C\tilde{x}(t)-LDw(t)-B_d d(t)\\&=(A(\alpha)+L(\alpha)C)\tilde{x}(t)+\begin{bmatrix}-L(\alpha)D&-B_d(\alpha)\end{bmatrix}n(t)\end{aligned} \tag{10}$$

where $n(t)=\begin{bmatrix}w(t)&d(t)\end{bmatrix}^T$.

Define

$$\xi(t)=\begin{bmatrix}x(t)\\\tilde{x}(t)\end{bmatrix} \tag{11}$$

Combining (9)–(10), we have

$$\begin{aligned}\dot{\xi}(t)&=\bar{A}(\alpha)\xi(t)+\bar{B}(\alpha)n(t)\\\tilde{y}(t)&=\bar{C}\xi(t)+\bar{D}n(t)\end{aligned} \tag{12}$$

where $\tilde{y}(t)$ is the output estimated error, and

$$\bar{A}=\begin{bmatrix}A(\alpha)+B(\alpha)K(\alpha)&B(\alpha)K(\alpha)\\0&A(\alpha)+L(\alpha)C\end{bmatrix},$$

$$\bar{B}=\begin{bmatrix}0&B_d(\alpha)\\-L(\alpha)D&-B_d(\alpha)\end{bmatrix},$$

$$\bar{C}=\begin{bmatrix}0&C\end{bmatrix},\bar{D}=\begin{bmatrix}-D&0\end{bmatrix}$$

Then, the design task of this paper can be further formulated as designing an observer-based state-feedback controller

$$u(t)=K(\alpha)\hat{x}(t) \tag{13}$$

such that (12) is stable and satisfies

$$\sigma_{max}(G(j\omega))<\gamma_1,\forall|\omega|\le\varpi_1 \tag{14}$$

where $G(j\omega)=\bar{C}(j\omega I-\bar{A}(\alpha))^{-1}\bar{B}(\alpha)+\bar{D}$ is the transfer function from $n(t)$ to $\tilde{y}(t)$.

Remark 1. Note that $K(\alpha)$ is a parameter-dependent controller gain matrix, and (14) is used to attenuate finite frequency disturbance $n(t)$.

Next, some lemmas are presented which are essential for the generation of LMI conditions for (14).

Lemma 1 ([19]). *Consider system (12), let symmetric matrix*

$$\Pi_1=\begin{bmatrix}I&0\\0&-\gamma_1^2 I\end{bmatrix} \tag{15}$$

be given, then condition

$$\sigma_{max}(G(j\omega))<\gamma_1,\forall|\omega|\le\varpi_1 \tag{16}$$

holds, if and only if

$$\begin{bmatrix}\bar{A}(\alpha)&I\\\bar{C}(\alpha)&0\end{bmatrix}\Xi(\alpha)\begin{bmatrix}\bar{A}(\alpha)&I\\\bar{C}(\alpha)&0\end{bmatrix}^T+\begin{bmatrix}\bar{B}(\alpha)&0\\\bar{D}(\alpha)&I\end{bmatrix}\Pi_1\begin{bmatrix}\bar{B}(\alpha)&0\\\bar{D}(\alpha)&I\end{bmatrix}^T<0 \tag{17}$$

holds, where

$$\Xi(\alpha)=\begin{bmatrix}-Q(\alpha)&P(\alpha)\\P(\alpha)&\varpi_1^2Q(\alpha)\end{bmatrix}$$

Proof. Similar to Lemma 1 of [27], the proof is omitted.

Lemma 2 ([34]). *Given U,V,Θ, there exists a matrix F such that*

$$UFV+(VFU)^T+\Theta<0 \tag{18}$$

holds, if and only if

$$N_U \Theta N_U^T < 0 \tag{19}$$

$$N_V^T \Theta N_V < 0 \tag{20}$$

hold simultaneously, where N_U and N_V are arbitrary matrices whose columns form a basis of the nulls paces of U and V, respectively.

Lemma 3. *Consider augmented system (12), let N_R be a null space matrix of R. The following statements are equivalent:*
(a) Condition (17) holds and

$$N_R^T(J\Xi(\alpha)J^T + H(\alpha)\Pi_1(\alpha)H(\alpha)^T)N_R < 0 \tag{21}$$

(b) The following inequality holds:

$$J\Xi(\alpha)J^T + H(\alpha)\Pi_1 H(\alpha)^T + L(\alpha)W(\alpha)R + (L(\alpha)W(\alpha)R)^T < 0 \tag{22}$$

where

$$J = \begin{bmatrix} I & 0 \\ 0 & I \\ 0 & 0 \end{bmatrix}, H(\alpha) = \begin{bmatrix} 0 & 0 \\ \bar{B}(\alpha) & 0 \\ \bar{D}(\alpha) & I \end{bmatrix}, L(\alpha) = \begin{bmatrix} -I \\ \bar{A}(\alpha) \\ \bar{C}(\alpha) \end{bmatrix}$$

and W is a positive definite matrix and $\Xi(\alpha)$ is defined in Lemma 1.

Proof. Let the null space matrix of $L(\alpha)$ be

$$N_L = \begin{bmatrix} \bar{A}(\alpha) & I & 0 \\ \bar{C}(\alpha) & 0 & I \end{bmatrix} \tag{23}$$

define

$$\Theta = J\Xi(\alpha)J^T + H(\alpha)\Pi_1(\alpha)H(\alpha)^T \tag{24}$$

Condition (17) in Lemma 1 is equivalent to

$$N_L \Theta N_L^T < 0 \tag{25}$$

according to Lemma 2, the conclusion is evident, this completes the proof.

Lemma 4 (*Young's Relation*)**.** *Given two matrices X and Y. Then, for any symmetric positive definite matrix S, condition*

$$X^TY + Y^TX \le X^TS^{-1}X + Y^TSY \tag{26}$$

holds.

Theorem 1. *Given augmented system (12), performance index*

$$\sigma_{max}(G(j\omega)) < \gamma_1, \forall|\omega| \le \varpi_1 \tag{27}$$

holds if the following LMI (28) holds,

$$\begin{bmatrix} -Q_{11}(\alpha) & -\bar{Q}_{12}(\alpha) & P_{11}(\alpha) - W_{11} & \bar{P}_{12}(\alpha) \\ * & -\bar{Q}_{22}(\alpha) & \bar{P}_{21}(\alpha) & \bar{P}_{22}(\alpha) - Y \\ * & * & T_1 & \varpi_1^2\bar{Q}_{12}(\alpha) \\ * & * & * & T_2 \\ * & * & * & * \\ * & * & * & * \\ * & * & * & * \\ * & * & * & * \\ * & * & * & * \end{bmatrix}$$

$$\begin{bmatrix} 0 & 0 & 0 & 0 & 0 \\ 0 & 0 & 0 & 0 & 0 \\ 0 & B(\alpha)\hat{K}(\alpha) & 0 & B_d(\alpha) & 0 \\ \hat{L}(\alpha)DD^T + C^T & 0 & I & -YB_d & \hat{L}D \\ DD^T - \gamma_1^2 I & 0 & 0 & 0 & 0 \\ * & -\frac{1}{\epsilon_1}W_{11} & 0 & 0 & 0 \\ * & * & -\epsilon_1 W_{11} & 0 & 0 \\ * & * & * & -I & 0 \\ * & * & * & * & -I \end{bmatrix} < 0 \tag{28}$$

where

$$T_1 = \varpi_1^2 Q_{11}(\alpha) + He(A(\alpha)W_{11} + B(\alpha)\hat{K}(\alpha))$$
$$T_2 = \varpi_1^2\bar{Q}_{22}(\alpha) + He(YA(\alpha) + \hat{L}(\alpha)C)$$

Proof.

$$R = \begin{bmatrix} 0 \\ I \\ 0 \end{bmatrix}^T, W = \begin{bmatrix} W_{11} & 0 \\ 0 & W_{22} \end{bmatrix},$$

$$Q(\alpha) = \begin{bmatrix} Q_{11}(\alpha) & Q_{12}(\alpha) \\ Q_{21}(\alpha) & Q_{22}(\alpha) \end{bmatrix}, P(\alpha) = \begin{bmatrix} P_{11}(\alpha) & P_{12}(\alpha) \\ P_{21}(\alpha) & P_{22}(\alpha) \end{bmatrix}$$

(22) can be rewritten as $\Lambda_1 < 0$, where

$$\Lambda_1 = \begin{bmatrix} -Q_{11}(\alpha) & -Q_{12}(\alpha) & P_{11}(\alpha) - W_{11} & P_{12}(\alpha) & 0 \\ * & -Q_{22}(\alpha) & P_{21}(\alpha) & P_{22}(\alpha) - W_{22} & 0 \\ * & * & S_1 & T_3 & 0 \\ * & * & * & S_2 & L(\alpha)DD^T + W_{22}^T C^T \\ * & * & * & * & DD^T - \gamma_1^2 I \end{bmatrix} \tag{29}$$

with

$$T_3 = \varpi_1^2 Q_{12}(\alpha) - B_d(\alpha)B_d^T(\alpha) + B(\alpha)K(\alpha)W_{22}$$
$$S_1 = \varpi_1^2 Q_{11}(\alpha) + B_d(\alpha)B_d^T(\alpha) + He(A(\alpha)W_{11} + B(\alpha)K(\alpha)W_{11})$$
$$S_2 = \varpi_1^2 Q_{22}(\alpha) + B_d(\alpha)B_d^T(\alpha) + L(\alpha)DD^TL^T(\alpha) + He(A(\alpha)W_{22} + L(\alpha)CW_{22})$$

Let $M_1 = diag\{I, I, I, Y, I\}$, $M_2 = diag\{I, Y, I, I, I\}$, performing a congruence transformation to (29), we have

$$M_1M_2\Lambda_1M_2^TM_1^T < 0 \tag{30}$$

where $Y = W_{22}^{-1}$, which is $\Lambda_2 < 0$, where

$$\Lambda_2 = \begin{bmatrix} -Q_{11}(\alpha) & -Q_{12}(\alpha)Y & P_{11}(\alpha) - W_{11} & P_{12}(\alpha)Y & 0 \\ * & -YQ_{22}(\alpha)Y & YP_{21}(\alpha) & YP_{22}(\alpha)Y - Y & 0 \\ * & * & S_1 & T_4 & 0 \\ * & * & * & S_3 & YL(\alpha)DD^T + C^T \\ * & * & * & * & DD^T - \gamma_1^2 I \end{bmatrix} \tag{31}$$

with

$$T_4 = \varpi_1^2 Q_{12}(\alpha)Y - B_d(\alpha)B_d^T(\alpha)Y + B(\alpha)K(\alpha)$$
$$S_3 = \varpi_1^2 YQ_{22}(\alpha)Y + YB_d(\alpha)B_d^T(\alpha)Y + YL(\alpha)DD^TL^T(\alpha)Y + He(YA(\alpha) + YL(\alpha)C)$$

Since (31) can be converted to

$$\Lambda_2 = \begin{bmatrix} -Q_{11}(\alpha) & -Q_{12}(\alpha)Y & P_{11}(\alpha) - W_{11} \\ * & -YQ_{22}(\alpha)Y & YP_{21}(\alpha) \\ * & * & S_1 \\ * & * & * \\ * & * & * \end{bmatrix}$$

$$\begin{bmatrix} P_{12}(\alpha)Y & 0 \\ YP_{22}(\alpha)Y - Y & 0 \\ T_5 & 0 \\ S_3 & YL(\alpha)DD^T + C^T \\ * & DD^T - \gamma_1^2 I \end{bmatrix} + \Upsilon_1 < 0 \tag{32}$$

where

$$T_5 = \varpi_1^2 Q_{12}(\alpha)Y - B_d(\alpha)B_d^T(\alpha)Y$$

and

$$\Upsilon_1 = \begin{bmatrix} 0 \\ 0 \\ BK(\alpha) \\ 0 \\ 0 \end{bmatrix} \begin{bmatrix} 0 \\ 0 \\ 0 \\ I \\ 0 \end{bmatrix}^T + \begin{bmatrix} 0 \\ 0 \\ 0 \\ I \\ 0 \end{bmatrix} \begin{bmatrix} 0 \\ 0 \\ BK(\alpha) \\ 0 \\ 0 \end{bmatrix}^T$$

Applying Lemma 4, we have

$$\begin{bmatrix} -Q_{11}(\alpha) & -Q_{12}(\alpha)Y & P_{11}(\alpha) - W_{11} & P_{12}(\alpha)Y & 0 \\ * & -YQ_{22}(\alpha)Y & YP_{21}(\alpha) & YP_{22}(\alpha)Y - Y & 0 \\ * & * & S_1 & T_5 & 0 \\ * & * & * & S_3 & YL(\alpha)DD^T + C^T \\ * & * & * & * & DD^T - \gamma_1^2 I \end{bmatrix} + \Upsilon_2 < 0 \tag{33}$$

where

$$\Upsilon_2 = \epsilon_1 \begin{bmatrix} 0 \\ 0 \\ BK(\alpha) \\ 0 \\ 0 \end{bmatrix} W_{11} \begin{bmatrix} 0 \\ 0 \\ BK(\alpha) \\ 0 \\ 0 \end{bmatrix}^T + \frac{1}{\epsilon_1} \begin{bmatrix} 0 \\ 0 \\ 0 \\ I \\ 0 \end{bmatrix} W_{11}^{-1} \begin{bmatrix} 0 \\ 0 \\ 0 \\ I \\ 0 \end{bmatrix}^T$$

and $\epsilon_1 > 0$. Let $\hat{K}(\alpha) = K(\alpha)W_{11}$, $\hat{L}(\alpha) = YL(\alpha)$, we get

$$\begin{bmatrix} -Q_{11}(\alpha) & -YQ_{12}(\alpha) & P_{11}(\alpha) - W_{11} & P_{12}(\alpha)Y \\ * & -YQ_{22}(\alpha)Y & YP_{21}(\alpha) & YP_{22}(\alpha)Y - Y \\ * & * & S_4 & T_5 \\ * & * & * & S_5 \\ * & * & * & * \\ * & * & * & * \\ * & * & * & * \end{bmatrix}$$
$$\begin{bmatrix} 0 & 0 & 0 \\ 0 & 0 & 0 \\ 0 & B(\alpha)\hat{K}(\alpha) & 0 \\ \hat{L}(\alpha)DD^T + C^T & 0 & I \\ DD^T - \gamma_1^2 I & 0 & 0 \\ * & -\frac{1}{\epsilon_1} W_{11} & 0 \\ * & * & -\epsilon_1 W_{11} \end{bmatrix} + \Upsilon_2 < 0 \tag{34}$$

where

$$S_4 = \varpi_1^2 Q_{11}(\alpha) + B_d(\alpha)B_d^T(\alpha) + He(A(\alpha)W_{11} + B(\alpha)\hat{K}(\alpha))$$

and

$$S_5 = \varpi_1^2 YQ_{22}(\alpha)Y + YB_d(\alpha)B_d^T(\alpha)Y + \hat{L}(\alpha)DD^T\hat{L}^T(\alpha) + He(YA(\alpha) + \hat{L}(\alpha)C)$$

Using Schur complement Lemma, and let

$$\bar{Q}_{12}(\alpha) = Q_{12}(\alpha)Y, \bar{Q}_{22}(\alpha) = YQ_{22}(\alpha)Y,$$
$$\bar{P}_{12}(\alpha) = P_{12}(\alpha)Y, \bar{P}_{21}(\alpha) = YP_{21}(\alpha),$$
$$\bar{P}_{22}(\alpha) = YP_{22}(\alpha)Y$$

we have that (28) holds.

4. Stability analysis

Firstly, the following lemma is essential for the formulation of stability conditions.

Lemma 5 ([35]). *For system (5), A is Hurwitz if there exist symmetric matrix variables X and W such that the following inequality holds:*

$$\begin{bmatrix} -(W + W^T) & W^TA^T + X & W^T \\ * & -X & 0 \\ * & * & -X \end{bmatrix} < 0 \tag{35}$$

where $V = W^{-1}$, $Y = X^{-1}$.

Theorem 2. *System (12) is stable if there exists positive scalar* ϵ_2, *and matrix variables* W_{11}, Y, $\bar{X}_{11}(\alpha)$, $\bar{X}_{12}(\alpha)$, $\bar{X}_{21}(\alpha)$, $\bar{X}_{22}(\alpha)$ *satisfying the following inequality*

$$\begin{bmatrix} -2W_{11} & 0 & T_6 & \bar{X}_{12}(\alpha) \\ * & -2Y & \bar{X}_{12}^T(\alpha) & T_7 \\ * & * & -\bar{X}_{11}(\alpha) & -\bar{X}_{12}(\alpha) \\ * & * & * & -\bar{X}_{22}(\alpha) \\ * & * & * & * \\ * & * & * & * \\ * & * & * & * \\ * & * & * & * \end{bmatrix}$$
$$\begin{bmatrix} W_{11}^T & 0 & 0 & 0 \\ 0 & Y & 0 & I \\ 0 & 0 & B(\alpha)\hat{K}(\alpha) & 0 \\ 0 & 0 & 0 & 0 \\ -\bar{X}_{11}(\alpha) & -\bar{X}_{12}(\alpha) & 0 & 0 \\ * & -\bar{X}_{22}(\alpha) & 0 & 0 \\ * & * & -\frac{1}{\epsilon_2} W_{11} & 0 \\ * & * & * & -\epsilon_2 W_{11} \end{bmatrix} < 0 \tag{36}$$

where

$$T_6 = \bar{X}_{11}^T(\alpha) + \hat{K}^T(\alpha)B^T(\alpha) + W_{11}^TA^T(\alpha)$$
$$T_7 = A^T(\alpha)Y^T + C^T\hat{L}^T(\alpha) + \bar{X}_{22}^T(\alpha)$$

Proof. Let

$$W = \begin{bmatrix} W_{11} & 0 \\ 0 & W_{22} \end{bmatrix}, X = \begin{bmatrix} X_{11}(\alpha) & X_{12}(\alpha) \\ X_{21}(\alpha) & X_{22}(\alpha) \end{bmatrix}$$

Apply Lemma 5, it is evident that (12) is stable if

$$\begin{bmatrix} -(W_{11} + W_{11}^T) & 0 & T_8 & X_{12}(\alpha) & W_{11}^T & 0 \\ * & -(W_{22} + W_{22}^T) & T_9 & T_{10} & 0 & W_{22}^T \\ * & * & -X_{11}(\alpha) & -X_{12}(\alpha) & 0 & 0 \\ * & * & * & -X_{22}(\alpha) & 0 & 0 \\ * & * & * & * & -X_{11}(\alpha) & -X_{12}(\alpha) \\ * & * & * & * & * & -X_{22}(\alpha) \end{bmatrix} < 0 \tag{37}$$

where

$$T_8 = W_{11}^TA^T(\alpha) + W_{11}^TK^T(\alpha)B^T(\alpha) + X_{11}(\alpha)$$
$$T_9 = W_{22}^TK^T(\alpha)B^T(\alpha) + X_{21}(\alpha)$$
$$T_{10} = W_{22}^TA^T(\alpha) + W_{22}^TC^TL^T(\alpha) + X_{22}(\alpha)$$

Define $Y = W_{22}^{-1}$, and let $M_3 = diag\{I, Y, I, Y, I, Y\}$, multiply (37) by M_3 and M_3^T on the left and right respectively, we have

$$\begin{bmatrix} -2W_{11} & 0 & T_8 & X_{12}(\alpha)Y & W_{11}^T & 0 \\ * & -2Y & T_{11} & T_{12} & 0 & Y \\ * & * & -X_{11}(\alpha) & -X_{12}(\alpha)Y & 0 & 0 \\ * & * & * & -YX_{22}(\alpha)Y & 0 & 0 \\ * & * & * & * & -X_{11} & -X_{12}(\alpha)Y \\ * & * & * & * & * & -YX_{22}(\alpha)Y \end{bmatrix} < 0 \tag{38}$$

where

$$T_{11} = K^T(\alpha)B^T(\alpha) + YX_{21}(\alpha),$$
$$T_{12} = A^T(\alpha)Y + C^TL^T(\alpha)Y + YX_{22}(\alpha)Y$$

Applying Lemma 4, it is obtained that (38) is equivalent to

$$\begin{bmatrix} -2W_{11} & 0 & T_{12} & X_{12}(\alpha)Y \\ * & -2Y & YX_{21}(\alpha) & T_{13} \\ * & * & -X_{11}(\alpha) & -X_{12}(\alpha)Y \\ * & * & * & -YX_{22}(\alpha)Y \\ * & * & * & * \\ * & * & * & * \\ * & * & * & * \\ * & * & * & * \end{bmatrix}$$
$$\begin{bmatrix} W_{11}^T & 0 & 0 & 0 \\ 0 & Y & 0 & I \\ 0 & 0 & B(\alpha)K(\alpha)W_{11} & 0 \\ 0 & 0 & 0 & 0 \\ -X_{11}(\alpha) & -X_{12}(\alpha)Y & 0 & 0 \\ * & -YX_{22}(\alpha)Y & 0 & 0 \\ * & * & -\frac{1}{\epsilon_2}W_{11} & 0 \\ * & * & * & -\epsilon_2 W_{11} \end{bmatrix} < 0 \quad (39)$$

where

$T_{12} = X_{11}^T(\alpha) + W_{11}^T K^T(\alpha) B^T(\alpha) + W_{11}^T A^T(\alpha)$

$T_{13} = A^T(\alpha)Y^T + C^T L^T(\alpha) Y + YX_{22}(\alpha)Y$

Let

$\bar{X}_{11}(\alpha) = X_{11}(\alpha), \bar{X}_{12}(\alpha) = X_{12}(\alpha)Y, \bar{X}_{22}(\alpha) = YX_{22}(\alpha)Y$

$\hat{K}(\alpha) = K(\alpha)W_{11}, \hat{L}(\alpha) = YL(\alpha)$

we have that (39) becomes (36), this completes the proof.

5. LMI conditions for controller design

The controller design problem is formulated as satisfying a set of LMIs, which can be solved readily.

Theorem 3. *Augmented system (12) is guaranteed to be stable and*

$$\sigma_{max}(G(j\omega)) < \gamma_1, \forall |\omega| \le \varpi_1 \quad (40)$$

is satisfied if there exist positive matrices $\bar{P}_i, W_{11}, Y$, matrices $\bar{Q}_i, \hat{L}_i, \hat{K}_i, A_j, B_j, B_{dj}$ and a positive scalar ϵ_1 satisfying the following LMIs for $i = 1, \ldots, 8, j = 1, \ldots, 8$

$$\Theta_{1ij} < 0 \quad (41)$$

$$\Theta_{2ij} < 0 \quad (42)$$

where

$$\Theta_{1ij} = \begin{bmatrix} -Q_{11i} & -\bar{Q}_{12i} & P_{11i} - W_{11} & \bar{P}_{12i} & 0 \\ * & -\bar{Q}_{22i} & \bar{P}_{21i} & \bar{P}_{22i} - Y & 0 \\ * & * & S_6 & \varpi_1^2 \bar{Q}_{12i} & 0 \\ * & * & * & S_7 & \hat{L}_i DD^T + C^T \\ * & * & * & * & DD^T - \gamma_1^2 I \\ * & * & * & * & * \\ * & * & * & * & * \\ * & * & * & * & * \\ * & * & * & * & * \end{bmatrix}$$
$$\begin{bmatrix} 0 & 0 & 0 & 0 \\ 0 & 0 & 0 & 0 \\ B_j\hat{K}_i & 0 & B_{dj} & 0 \\ 0 & I & -YB_{dj} & \hat{L}_i D \\ 0 & 0 & 0 & 0 \\ -\frac{1}{\epsilon_1}W_{11} & 0 & 0 & 0 \\ * & -\epsilon_1 W_{11} & 0 & 0 \\ * & * & -I & 0 \\ * & * & * & -I \end{bmatrix} \quad (43)$$

$$\Theta_{2ij} = \begin{bmatrix} -2W_{11} & 0 & S_8 & \bar{X}_{12i} & W_{11}^T & 0 & 0 & 0 \\ * & -2Y & \bar{X}_{12i}^T & S_9 & 0 & Y & 0 & I \\ * & * & -\bar{X}_{11} & -\bar{X}_{12i} & 0 & 0 & B_j\hat{K}_i & 0 \\ * & * & * & -\bar{X}_{22i} & 0 & 0 & 0 & 0 \\ * & * & * & * & -\bar{X}_{11} & -\bar{X}_{12i} & 0 & 0 \\ * & * & * & * & * & -\bar{X}_{22i} & 0 & 0 \\ * & * & * & * & * & * & -\frac{1}{\epsilon_2}W_{11} & 0 \\ * & * & * & * & * & * & * & -\epsilon_2 W_{11} \end{bmatrix} \quad (44)$$

where

$S_6 = \varpi_1^2 Q_{11i} + He(A_j W_{11} + B_j\hat{K}_i), S_7 = \varpi_1^2 \bar{Q}_{22i} + He(YA_j + \hat{L}_i C)$

$S_8 = \bar{X}_{11i}^T + \hat{K}_i^T B_j^T + W_{11}^T A_j^T, S_9 = A_j^T Y^T + C^T \hat{L}_i^T + \bar{X}_{22}^T$

Proof. Note that

$A(\alpha) = \sum_{j=1}^8 \alpha_j A_j, B(\alpha) = \sum_{j=1}^8 \alpha_j B_j,$

$B_d(\alpha) = \sum_{j=1}^8 \alpha_j B_{dj}.$

Let

$$Q_{11}(\alpha) = \sum_{i=1}^8 \alpha_i Q_{11i}, Q_{12}(\alpha) = \sum_{i=1}^8 \alpha_i Q_{12i}, Q_{21}(\alpha) = \sum_{i=1}^8 \alpha_i Q_{21i},$$

$$Q_{22}(\alpha) = \sum_{i=1}^8 \alpha_i Q_{22i}, P_{11}(\alpha) = \sum_{i=1}^8 \alpha_i P_{11i}, P_{12}(\alpha) = \sum_{i=1}^8 \alpha_i P_{12i},$$

$$P_{21}(\alpha) = \sum_{i=1}^8 \alpha_i P_{21i}, P_{22}(\alpha) = \sum_{i=1}^8 \alpha_i P_{22i}, K(\alpha) = \sum_{i=1}^8 \alpha_i K_i,$$

$$\hat{K}(\alpha) = \sum_{i=1}^8 \alpha_i \hat{K}_i, L(\alpha) = \sum_{i=1}^8 \alpha_i L_i, \hat{L}(\alpha) = \sum_{i=1}^8 \alpha_i \hat{L}_i$$

we have that (28) is equivalent to

$$\sum_{i=1}^8 \sum_{j=1}^8 \alpha_i \alpha_j \Theta_{1ij} < 0 \quad (45)$$

Obviously, performance index (40) is satisfied if (41) holds for $i = 1, \ldots, 8$. Similarly, system (12) is guaranteed to be stable if (42) holds for $i = 1, \ldots, 8$, this completes the proof.

From Theorem 3, we have that the controller gains can be calculated by solving the following convex optimization problem

$$\begin{aligned} &\min \ \gamma_1 \\ &s.t. \ (41), (42) \end{aligned} \quad (46)$$

where $i = 1, \ldots, 8, j = 1, \ldots, 8$.

6. Simulation results

In this section, the proposed design method is verified through an AGV model, whose parameters are $m = 1573$ kg, $I_z = 2873$ kg m^2, $l_f = 1.1$ m, $l_r = 1.58$ m, $C_f = 80\,000$ N/rad, $C_r = 80\,000$ N/rad. Assume that the velocity v_x varies in [15, 25], the frequency parameter $\omega_1 = 8$, positive constant $\epsilon_1 = 0.01, \epsilon_2 = 0.02$. Through solving (46), the $H\infty$ performance index is obtained to be $\gamma = 0.0844$, the controller gain K_i and observer gain L_i are obtained simultaneously, and $K(\alpha) = \sum_{i=1}^8 \alpha_i K_i, L(\alpha) = \sum_{i=1}^8 \alpha_i L_i$ are both parameter-dependent, for example, when $v_x = 20$ m/s, we have

$$K = \begin{bmatrix} -0.1091 & -3.1639 & -0.7469 & -0.5890 \end{bmatrix},$$

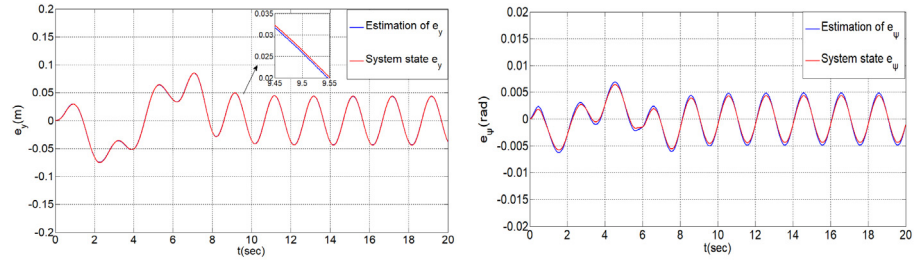

(a) Responding curves of e_y (b) Responding curves of e_ψ

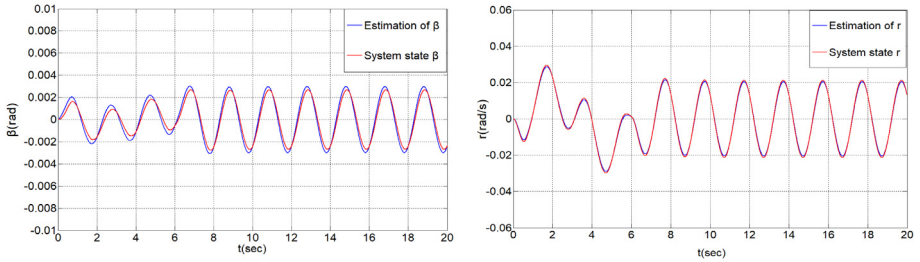

(c) Responding curves of sideslip angle β (d) Responding curves of yaw rate r

Fig. 2. Simulation results of system states. (For interpretation of the references to color in this figure legend, the reader is referred to the web version of this article.)

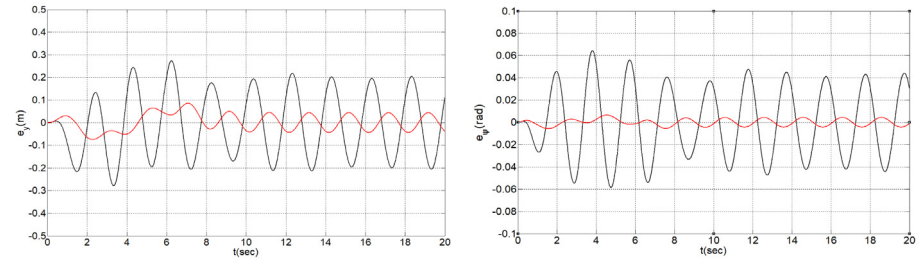

(a) Responding curves of e_y without using observer (black line) and using observer (red line) (b) Responding curves of e_ψ without using observer (black line) and using observer (red line)

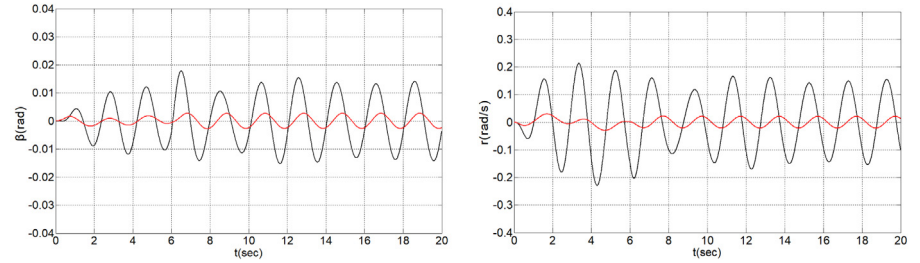

(c) Responding curves of β without using observer (black line) and using observer (red line) (d) Responding curves of r without using observer (black line) and using observer (red line)

Fig. 3. Responding curves of system states without using observer (black line) and using observer (red line). (For interpretation of the references to color in this figure legend, the reader is referred to the web version of this article.)

$$L = 10^3 \times \begin{bmatrix} -0.2928 & -0.0409 & -0.0181 & -0.0057 \\ 0.0077 & -1.0817 & -0.0123 & -0.0068 \\ -0.0138 & 0.0004 & -0.0345 & -0.0043 \\ -0.0092 & 0.0001 & -0.0188 & -0.0215 \end{bmatrix}$$

Assume that initial state $x_0 = [0, 0, 0, 0]^T$, external disturbance $d(t)$=[0.01sin(πt), 0.001 sin(πt)− ρ,0.01 sin(πt), 0.02 sin(πt)]^T, measurement noise $w(t) = \sin(\pi t)\times$ [0.01, 0.01, 0.02, 0.01]^T. v_x is variable, which is assumed to be $v_x = 16$ m/s for $t \leq 6$ s, $v_x = 20$ m/s for $6 < t \leq 13$ s, and $v_x = 24$ m/s for $t > 13$ s. Fig. 2 show the state estimation results, where the red lines denote the true values, and the blue lines denote the estimation results of the observer.

In order to verify the advantage of the approach proposed, we compare the finite frequency observer-based controller with the finite frequency controller without observer and full frequency observer-based controller, respectively. Firstly, Fig. 3 show the comparison results of state estimation for the finite frequency

Table 1
Comparison results of path tracking errors e_y and heading angle errors e_ψ using full frequency observer based method and finite frequency observer based method under different levels of noises.

Noises level	Root mean square of e_y		Root mean square of e_ψ	
	Full frequency	Finite frequency	Full frequency	Finite frequency
M = 0.05	0.0363	0.028	0.0042	0.0017
M = 0.1	0.1356	0.1022	0.0292	0.0219
M = 1	0.311	0.2304	0.0639	0.047
M = 3	1.0172	0.748	0.2033	0.1476

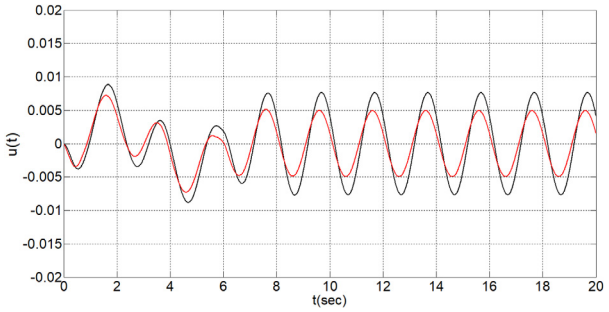

Fig. 4. Control input. The control inputs of finite frequency approach and full frequency approach are denoted by the red line and the black line respectively. (For interpretation of the references to color in this figure legend, the reader is referred to the web version of this article.)

control approaches with and without observer, respectively, from which we have that the observer-based state-feedback control approach receives better results.

To compare with the classic full frequency observer-based state-feedback controller design condition, which is provided in Lemma 6 of Appendix, solving optimization problem (46) with conditions (41)–(42) being replaced by (48), we have $H\infty$ performance index $\gamma = 0.4411$, the controller gain $K(\alpha)$ and $L(\alpha)$ for full frequency approach can also be calculated, and when $v_x = 20$ m/s, we have

$$K = \begin{bmatrix} -0.0748 & -0.9398 & -0.4242 & -0.0699 \end{bmatrix}$$

$$L = 10^3 \times \begin{bmatrix} -0.1471 & -0.0396 & -0.0438 & -0.0228 \\ -0.0381 & -1.9453 & -0.0063 & -0.0033 \\ -0.0436 & -0.0050 & -0.0459 & -0.0171 \\ -0.0230 & -0.0023 & -0.0173 & -0.0190 \end{bmatrix}$$

Fig. 4 shows curves of control inputs of both approaches, and Fig. 5 shows comparison results of state estimation, where the red lines denote the state estimation results of finite frequency approach and black line denote the state estimation results of full frequency approach, obviously, the finite frequency approach generates smaller estimation error and sideslip angle.

Furthermore, to see the results from different levels of noises, let $w(t) = M \times [\sin(\pi t), \sin(\pi t), \sin(\pi t), \sin(\pi t)]^T$, where M is a positive scalar, the comparison results for different M are shown in Table 1, which shows that the controller designed receives better results than existing full frequency methods.

To see the path tracking results, suppose that a single-lane change is completed at 20 m/s. The road curvature is plotted in Fig. 6, and the global trajectories of the AGV using different approaches are shown in Fig. 7, where the desired trajectory is denoted by blue line, the vehicle trajectory generated by using the full frequency observe-based $H\infty$ control method is denoted by black line, while the vehicle trajectory generated by the method of this paper is denoted by red line, which receives better results.

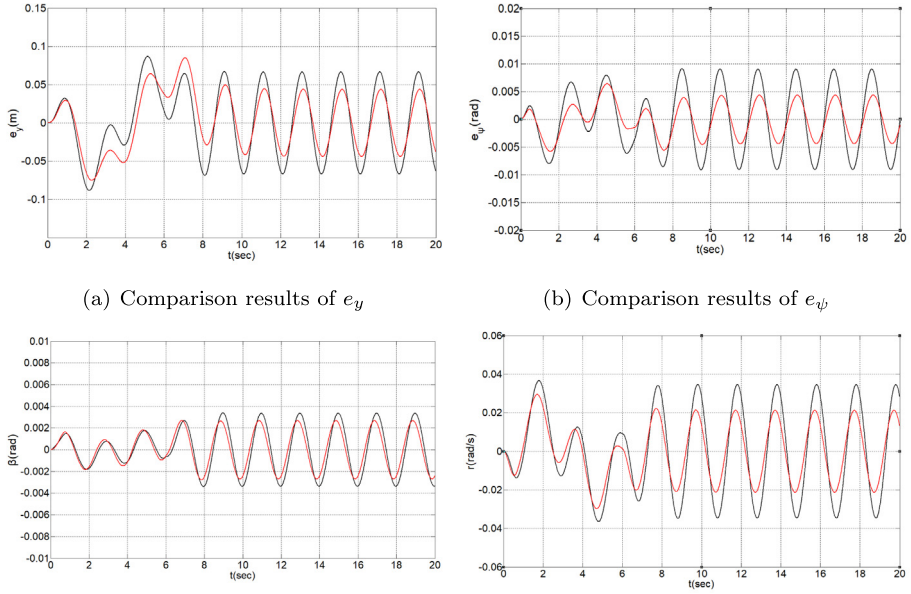

(a) Comparison results of e_y

(b) Comparison results of e_ψ

(c) Comparison results of β

(d) Comparison results of r

Fig. 5. Comparison results of system states between full frequency observer-based state-feedback control approach (black line) and finite frequency observer-based state-feedback control approach (red line). (For interpretation of the references to color in this figure legend, the reader is referred to the web version of this article.)

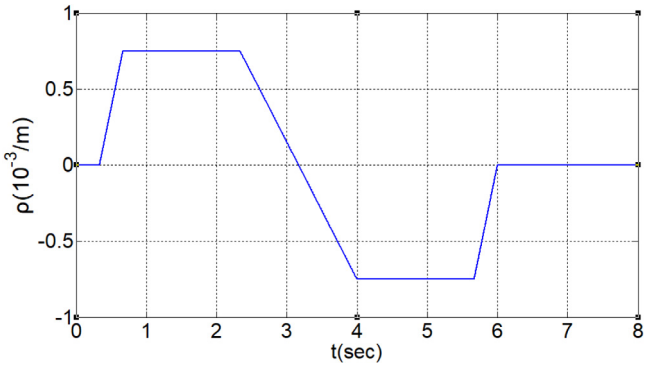

Fig. 6. Simulation results of the road curvature in single-lane change maneuver.

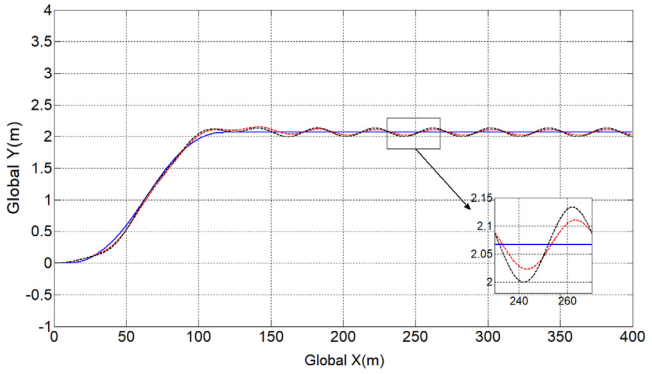

Fig. 7. Global trajectories for single-lane change maneuver. (For interpretation of the references to color in this figure legend, the reader is referred to the web version of this article.)

To further demonstrate the effectiveness of the method proposed, a double-lane change maneuver is tested in CarSim simulation environment [24,25], Fig. 8 shows the simulation environment, and Fig. 9 shows the state responding curves for both the full frequency and finite frequency methods, where the finite frequency method proposed in this paper receives better results.

7. Conclusions

In this paper, the path tracking control problem of AGVs is considered, an finite frequency observer-based control method is proposed, where the closed-loop control system is stable and certain finite frequency performances are satisfied. The nonlinear AGV model is transformed into an LPV system, and both the parameter-dependent controller gains and parameter-dependent observer gains are determined simultaneously through solving a convex optimization problem. Simulation results shows the effectiveness of the design method proposed, and the advantage of the proposed method has been illustrated through comparing with existing classic full frequency design problem.

Declaration of competing interest

The authors declare that they have no known competing financial interests or personal relationships that could have appeared to influence the work reported in this paper.

Fig. 8. Simulation environment in CarSim for double-lane change maneuver of an AGV.

Appendix

Lemma 6. *System (12) is stable with condition*

$$\sigma_{max}(G(j\omega)) < \gamma_1 \tag{47}$$

if there exist positive matrices P_{22}, Y, *matrices* $\hat{L}_i, \hat{K}_i, A_j, B_j, B_{dj}$ *and a positive scalar* ϵ_3 *such that*

$$\begin{bmatrix} He(A_jY + B_j\hat{K}_i) & 0 \\ * & He(P_{22}A_j + \hat{L}_iC) \\ * & * \\ * & * \\ * & * \\ * & * \\ * & * \end{bmatrix}$$

$$\begin{bmatrix} 0 & B_{dj} & 0 & B_j\hat{K}_i & 0 \\ -\hat{L}_iD & -P_{22}B_{dj} & C^T & 0 & I \\ -\gamma^2 I & 0 & -D^T & 0 & 0 \\ * & -\gamma^2 I & 0 & 0 & 0 \\ * & * & -I & 0 & 0 \\ * & * & * & -\frac{1}{\epsilon_3}Y_i & 0 \\ * & * & * & * & -\epsilon_3 Y_i \end{bmatrix} < 0 \tag{48}$$

holds for $i = 1, \ldots, 8$.

Proof. Applying Bounded Real Lemma, it can be easily obtained that (47) is satisfied if

$$\begin{bmatrix} \bar{A}^T(\alpha)P + P\bar{A}(\alpha) & P\bar{B}(\alpha) & \bar{C}^T \\ * & -\gamma^2 I & \bar{D}^T \\ * & * & -I \end{bmatrix} < 0 \tag{49}$$

holds. Let

$$P = \begin{bmatrix} P_{11} & 0 \\ 0 & P_{22} \end{bmatrix} < 0$$

Define $M_4 = diag\{Y, I, I, I, I\}$, multiply (49) by M_4 and M_4^T on the left and right sides respectively, we have

$$\begin{bmatrix} He(A(\alpha)Y + B(\alpha)\hat{K}(\alpha)) & B(\alpha)K(\alpha) \\ * & He(P_{22}A(\alpha) + \hat{L}(\alpha)C) \\ * & * \\ * & * \\ * & * \end{bmatrix}$$

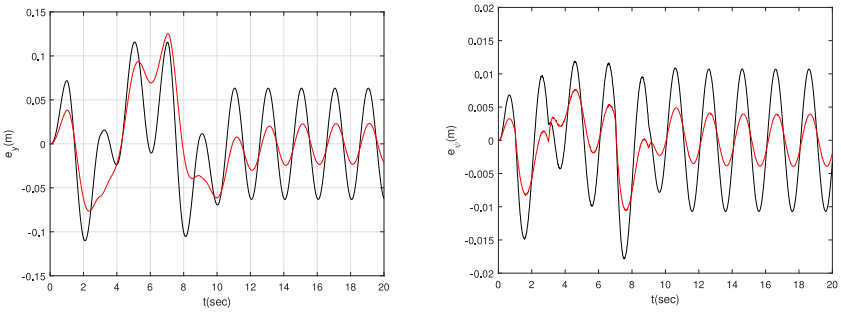

(a) Responding curves of e_y

(b) Responding curves of e_ψ

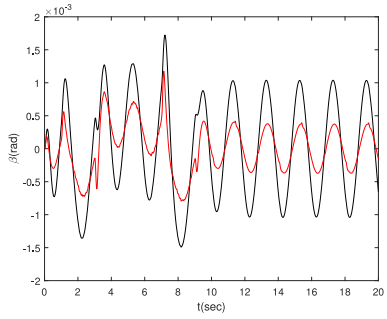

(c) Responding curves of β

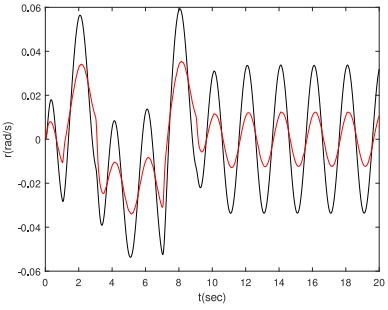

(d) Responding curves of r

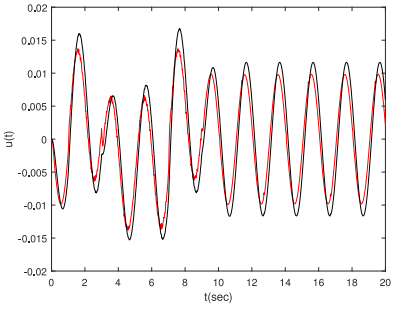

(e) Responding curves of u

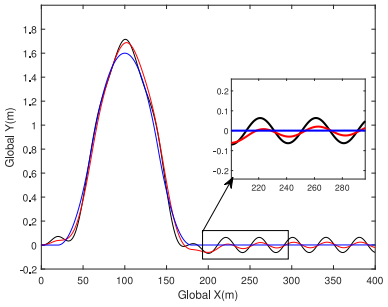

(f) Simulation results of global trajectories

Fig. 9. State responding curves for double-lane change using full frequency observer-based state-feedback control approach (black lines) and finite frequency observer-based state-feedback control approach (red lines). (For interpretation of the references to color in this figure legend, the reader is referred to the web version of this article.)

$$\begin{bmatrix} 0 & B_d(\alpha) & 0 \\ -\hat{L}(\alpha)D & -P_{22}B_d(\alpha) & C^T \\ -\gamma^2 I & 0 & -D^T \\ * & -\gamma^2 I & 0 \\ * & * & -I \end{bmatrix} < 0 \tag{50}$$

where $Y = P_{11}^{-1}$, $\hat{L}(\alpha) = P_{22}L(\alpha)$, $\hat{K}(\alpha) = K(\alpha)Y$. Using Lemma 4, we have

$$\begin{bmatrix} He(A(\alpha)Y + B(\alpha)\hat{K}(\alpha)) & 0 \\ * & He(P_{22}A(\alpha) + \hat{L}(\alpha)C) \\ * & * \\ * & * \\ * & * \\ * & * \\ * & * \end{bmatrix}$$

$$\begin{bmatrix} 0 & B_d(\alpha) & 0 & B(\alpha)\hat{K}(\alpha) & 0 \\ -\hat{L}(\alpha)D & -P_{22}B_d(\alpha) & C^T & 0 & I \\ -\gamma^2 I & 0 & -D^T & 0 & 0 \\ * & -\gamma^2 I & 0 & 0 & 0 \\ * & * & -I & 0 & 0 \\ * & * & * & -\frac{1}{\epsilon_3}Y(\alpha) & 0 \\ * & * & * & * & -\epsilon_3 Y(\alpha) \end{bmatrix} < 0 \tag{51}$$

Similar to Theorem 2, we have if (48) holds for $i = 1, \ldots, 8$, (51) holds, this completes the proof.

References

[1] Tang Z, Xu X, Wang F, Jiang XW, Jiang HB. Coordinated control for path following of two-wheel independently actuated autonomous ground vehicle. IET Intell Transp Syst 2019;13(4):628–35.
[2] Cui L, Wei Y, Wang YY. Finite-time trajectory tracking control for autonomous airships with uncertainties and external disturbances. IET Intell Transp Syst 2020;14(5):440–8.
[3] Peppard LE. String stability of relative-motion PID vehicle control systems. IEEE Trans Autom Control 1974;19(5):579–81.

[4] Ang KH, Chong G, Li Y. PID control system analysis, design, and technology. IEEE Trans Control Syst Technol 2005;13(4):559–76.
[5] Rosolia U, Bruyne SD, Alleyne AG. Autonomous vehicle control: a non-convex approach for obstacle avoidance. IEEE Trans Control Syst Technol 2016;25(2):1–16.
[6] Yu J, Guo X, Pei X, Chen Z, Wu C. Path tracking control based on tube MPC and time delay motion prediction. IET Intell Transp Syst 2020;14(1):1–12.
[7] Wang Z, Li G, Jiang H, Chen Q, Zhang H. Vehicle steering control with MPC for target trajectory tracking of autonomous reverse parking. IEEE/ASME Trans Mechatronics 2018;23(3):1103–13.
[8] Huang Y, Wang H, Khajepour A, Ding H, Qin Y. A novel local motion planning framework for autonomous vehicles based on resistance network and model predictive control. IEEE Trans Veh Technol 2020;69(1):55–66.
[9] Xu S, Peng H. Design, analysis, and experiments of preview path tracking control for autonomous vehicles. IEEE Trans Intell Transp Syst 2020;21(1):48–58.
[10] Hwang CL, Yang CC, Hung JY. Path tracking of an autonomous ground vehicle with different payloads by hierarchical improved fuzzy dynamic sliding-mode control. IEEE Trans Fuzzy Syst 2018;26(2):899–914.
[11] Wang D, Lian J, Ge YL, Wang W. Sliding mode control for switched nonlinear systems under asynchronous switching. In: IEEE international conference on systems, man, and cybernetics. 2014, p. 3272–7.
[12] Guo B, Chen Y. Robust adaptive fault-tolerant control of four-wheel independently actuated electric vehicles. IEEE Trans Ind Inform 2020;16(5):2882–94.
[13] Wu Y, Wang L, Zhang J, Li F. Andréanovel b.d.: 'path following control of autonomous ground vehicle based on nonsingular terminal sliding mode and active disturbance rejection control. IEEE Trans Veh Technol 2019;68(7):6379–90.
[14] Li WF, Xie ZC, Zhao J, Wong PK. Velocity-based robust fault tolerant automatic steering control of autonomous ground vehicles via adaptive event triggered network communication. Mech Syst Signal Process 2020;143:1–19.
[15] Ji XW, He XK, Lv C, Liu YH, Wu J. Adaptive-neural-network-based robust lateral motion control forautonomous vehicle at driving limits. Mech Syst Signal Process 2018;76:41–53.
[16] Lee YS, Moon YS, Kwon WH. Delay-dependent robust H∞ control for uncertain systems with a state-delay. Automatica 2004;40(1):65–72.
[17] Wang RR, Jing H, Hu C, Yan FJ, Chen N. Adaptive fault-tolerant tracking control of 4WS4WD road vehicles: A fully model-independent solution. IEEE Trans Intell Transp Syst 2016;17(7):2042–50.
[18] Hu XX, Karimi HR, Gao HJ, Hu CH. Fuzzy non-fragile H∞ tracking control for flexible air-breathing hypersonic vehicles. IFAC Proc Vol 2012;45(4):242–7.
[19] Iwasaki T, Kara S. Generalized KYP lemma: unified frequency domain inequalities with design applications. IEEE Trans Autom Control 2005;50(1):41–59.
[20] Sun WC, Gao HJ, Kaynak O. Finite frequency control for vehicle active suspension systems. IEEE Trans Control Syst Technol 2011;19(2):416–22.
[21] Qiu J, Ren M, Zhao Y, Guo Y. Active fault-tolerant control for vehicle active suspension systems in finite-frequency domain. IET Control Theory Appl 2011;5(13):1544–50.
[22] Guo H, Chen H, Cao D, Jin W. Design of a reduced-order nonlinear observer for vehicle velocities estimation. IET Control Theory Appl 2013;7(17):2056–68.
[23] Guo H, Cao D, Chen H, Sun ZP. Model predictive path following control for autonomous cars considering a measurable disturbance: Implementation, testing, and verification. Mech Syst Signal Process 2019;118:41–60.
[24] Wang R, Jing H, Hu C, Yan F, Chen N. Robust H∞ path following control for autonomous ground vehicles with delay and data dropout. IEEE Trans Intell Transp Syst 2016;17(7):2042–50.
[25] Wang JX, Wang JM, Wang RR, Hu C. A framework of vehicle trajectory replanning in lane exchanging with considerations of driver characteristics. IEEE Trans Veh Technol 2017;66(5):3583–96.
[26] He X, Zhao J. Switching stabilization and H∞ performance of a class of discrete switched LPV system with unstable subsystems. Nonlinear Dyn 2014;76(2):1069–77.
[27] Wang H, Yang GH. Integrated fault detection and control for LPV systems. Int J Robust Nonlinear Control 2009;19(3):341–63.
[28] Xie W. H2 gain scheduled state feedback for LPV system with new LMI formulation. IEEE Proc - Control Theory Appl 2005;152(6):693–7.
[29] Zhang BJ, Du HP, Lam J, Zhang N, Li WH. A novel observer design for simultaneous estimation of vehicle steering angle and sideslip angle. IEEE Trans Ind Electron 2016;63(7):4357–66.
[30] Donald S, Matteo C, Giulio P, Sergio MS. Vehicle sideslip estimation: A kinematic based approach. Control Eng Pract 2017;67:1–12.
[31] Chu ZZ, Zhu DQ, Yang SX. Observer-based adaptive neural network trajectory tracking control for remotely operated vehicle. IEEE Trans Neural Netw Learn Syst 2016;28(7):1–13.
[32] Zhang C, Hu J, Qiu J, Yang W, Sun H, Chen Q. A novel fuzzy observer-based steering control approach for path tracking in autonomous vehicles. IEEE Trans Fuzzy Syst 2019;27(2):278–90.
[33] Zhang H, Zhang G, Wang J. H∞ observer design for LPV systems with uncertain measurements on scheduling variables: Application to an electric ground vehicle. IEEE/ASME Trans Mechatronics 2016;21(3):1659–70.
[34] Liu C, Li L, Yong J, Muhammad F, Cheng S. An innovative finite frequency H∞ observer for radar tracking. IEEE Trans. Intell Transp Syst 2020;1–9.
[35] Apkarian P, Tuan HD, Bernussou J. Analysis, eigenstructure assignment and h2 multichannel synthesis with enhanced LMI characterizations. In: IEEE conference on decision & control. 2000, p. 1489–94.